Extrinsic contributions to the apparent thickness dependence of the dielectric constant in epitaxial $Pb(Zr,Ti)O_3$ thin films

L. Pintilie
NIMP, P.O. Box MG-7, 077125 Bucharest-Magurele, Romania and Max Planck Institute of Microstructure Physics, Weinberg 2, 06120 Halle, Germany

I. Vrejoiu, D. Hesse, G. LeRhun, and M. Alexe
Max Planck Institute of Microstructure Physics, Weinberg 2, 06120 Halle, Germany

(Received 28 August 2006; revised manuscript received 25 May 2007; published 20 June 2007)

The problem of the thickness dependence of the dielectric constant, as well as the extrinsic contributions to its value, is analyzed for the case of epitaxial $Pb(Zr,Ti)O_3$ (PZT) thin films. It is shown that the frequency dependence of the measured capacitance is best simulated by an equivalent circuit incorporating the trap-containing capacitance of a Schottky contact. The thickness dependence of the dielectric constant, calculated using the formula of a plane capacitor, *appears* to be an extrinsic effect due to the interface phenomena in the metal-ferroelectric-metal structure. The intrinsic dielectric constant of the PZT material seems to be thickness independent and of low value of about 30–40. This is closer to the values estimated from Raman measurements or from quantum theories of ferroelectricity. The thickness independence is also proven by piezoresponse force microscopy measurements. The presence of traps is evidenced by the presence of a photovoltaic effect at subgap wavelengths.

DOI: 10.1103/PhysRevB.75.224113 PACS number(s): 77.80.−e, 73.40.Sx, 77.84.Dy

I. INTRODUCTION

The static or low-frequency dielectric constant, shortly named “dielectric constant,” is an important quantity in the case of ferroelectric materials of $Pb(Zr,Ti)O_3$ (PZT) type.[1] Its knowledge is important in the case of designing electronic components or modeling electric and ferroelectric properties.[2] The main problem is the large spread of the reported values, especially in the case of thin films, although the PZT composition is the same. This fact raises serious problems when attempting to place numerical values for the dielectric constant into theoretical models simulating the experimental results. For example, the thermodynamic theory predicts that the dielectric constant along the polar axis is 67 for $PbTiO_3$ (PTO) and 86 for PZT with a Zr/Ti ratio of 20/80, a much studied composition in recent years.[3] Raman measurements performed on $PbTiO_3$ crystals, coupled with the Lyddane-Sachs-Teller (LST) relation, give a value of 41 for the static dielectric constant.[4] More recent quantum theories predict a value of about 40.[5,6] On the other hand, the reported values for the dielectric constant extracted from capacitance measurements, for similar PZT compositions, vary from about 320 (Ref. 7) to about 120 (Ref. 8), going through some other values in the 200–300 range.[9–11] Discrepancies in the values of the dielectric constant were reported earlier, for other ABO_3 perovskite compounds, such as $BaTiO_3$, $LiTaO_3$, or $Pb_{1-x}La_xTi_{1-x/4}O_3$.[12] For these compounds it was observed that the dielectric constant evaluated from the lattice vibration modes (ε_m) is smaller than the dielectric constant evaluated from capacitance measurements (ε_{cap}). The difference was attributed to relaxation mechanisms which are active at the low frequencies used for capacitance measurements (usually in the range of 10^2-10^6 Hz), but are not active in the frequency range used for Raman measurements (which are larger than 10^{10} Hz). Such mechanisms could be related to the presence of impurities, structural disorder, composition fluctuations, etc. It was observed that the ratio $\varepsilon_{cap}/\varepsilon_m$ increases in the materials with a higher degree of disorder, while it is close to 1 in single crystals such as $LiTaO_3$ or $LiNbO_3$.[13] A theory of “dirty” displacive ferroelectrics was developed, considering the coupling between impurities and lattice modes.[14] However, the theory does not take into account the fact that the structure used for capacitance measurements is a metal-ferroelectric-metal (MFM) structure, while for optic measurements the electrodes are missing. Therefore, the interface effects are not considered. The temperature- and time-dependent electron exchange between charged structural defects and the electron bands was also neglected.[15] It is interesting to observe that, with few exceptions, the effect of the microstructure on the dielectric behavior was disregarded. An exception was the above mentioned theory of dirty displacive ferroelectrics, which tried to reconcile the dielectric constant derived from electric measurements of the capacitance with the soft-mode models of ferroelectricity. Other exceptions are related to the ferroelectric domain walls, which are structural defects that can bring significant extrinsic contributions to the dielectric constant derived from capacitance measurements performed at small electric fields.[16–20] However, most real samples are full of other defects, such as vacancies, impurities, dislocations, and grain boundaries, not to mention the electrode interfaces. All these can contribute in different ways to the dielectric response—i.e., to the dielectric constant.[21,22]

Closely related to this spread of values over two orders of magnitude, as exemplified for PZT20/80, is the so-called “thickness dependence” of the dielectric constant. It was found that the latter decreases with decreasing thickness of PZT ferroelectric films.[23,24] This is usually explained by the

 ©2007 The American Physical Society

presence of a thin layer of low dielectric constant at the electrode interfaces (the "dead layer"), leading to the series capacitor model suggested by Scott *et al.*[25] Later on theories were developed to sustain the presence of the dead layer and thickness dependence of the dielectric constant.[26–32] Recently it was shown that thickness effects, such as the "smearing" of the ferroelectric transition and the thickness dependence of the dielectric constant and transition temperature, are not intrinsic phenomena in the case of $BaTiO_3$ (BTO), $SrTiO_3$ (STO), and $(Ba_{0.5}Sr_{0.5})TiO_3$ (BST) single-crystalline thin films.[33–35] It was shown that, with a proper data analysis, the transition temperature is thickness independent in the case of the BTO and BST samples and that the dielectric constant is close to that of the bulk in the case of STO layers. However, it might be not appropriate to compare results, or to extend models and conclusions, from BTO-STO-type materials to PTO or Ti-rich PZT layers. In spite of the same ABO_3 type and tetragonal-to-cubic transition, the materials might be very different in behavior. This statement is based on the fact that the *A*-O bond has a very different nature in BTO and PTO (or Ti-rich PZT). It was experimentally observed that the perovskite compounds with smaller covalent bond energy of the *A*-O bonds have a higher transition temperature.[36] Later on it was theoretically argued that the Ba-O bond is ionic, whereas the Pb-O bond is covalent.[37] In other words, in the case of the Ba-O bond the electrons are localized and the bond is polar, while in the case of the Pb-O bond the electrons are delocalized. The electron-lattice interaction then contributes to the stability of the ferroelectric phase at higher temperatures. This important difference can have significant consequences for the electronic properties of the two types of materials. Therefore, the models used to explain the properties of the BTO-BST system might not be valid in the case of the PTO-PZT system, including the models developed to explain the thickness effects.

Returning to the problem of the dead layer in MFM structures, as a layer of different properties, recent experimental investigations on epitaxial PZT do not support its presence in this case.[38] However, the presence of an interfacial capacitance cannot be totally ruledout as it seems that in PZT epitaxial films it is more appropriate to use the Schottky model for the metal-ferroelectric interfaces, including the voltage-dependent Schottky capacitance.[39–41] The present paper will produce further evidence that, in the specific case of epitaxial Ti-rich PZT films, the Schottky model is more appropriate.

Experimentally, the dielectric constant is measured using a simple plane-parallel capacitor geometry and is determined using the following relation:

$$C_m = \varepsilon_0 \varepsilon \frac{S}{d}, \tag{1}$$

where C_m is the measured capacitance, ε_0 is the vacuum permittivity, ε is the dielectric constant, S is the capacitor area, and d is the thickness. However, different experimental values are obtained for a structure with Schottky contacts if the dielectric constant is simply calculated using the above formula. The most known example is silicon which has a textbook value of its dielectric constant of 11.9 and any developed model uses it.[42] Attempts to use Eq. (1) to calculate the dielectric constant of Si will fail. It can be easily shown that the "dielectric constant" calculated in this way is given by the product between the intrinsic dielectric constant and a d/w factor, where d is the thickness of the sample and w is the thickness of the depleted region of the Schottky diode. As usually $d > w$, the dielectric constant calculated using Eq. (1) will be larger than the intrinsic value. Only in the particular case of full depletion, when $d \leq w$, is the dielectric constant calculated from the planar capacitor identical to the dielectric constant of the material of the Schottky diode.

We can extrapolate the above example to PZT epitaxial films and we can state that there is a problem related to determining the dielectric constant of PZT by simply using Eq. (1). The quantity calculated using the above formula of a planar capacitor applied to a MFM structure might be far from the intrinsic value of the ferroelectric material.

In this paper we analyze the problem of the dielectric constant in epitaxial tetragonal PZT films with special emphasis on its thickness dependence and on the intrinsic-extrinsic contributions. We assume that the depletion layers at the metal-ferroelectric Schottky contacts significantly contribute to the measured capacitance and we consider them in a simple model which allows for an evaluation of the intrinsic permittivity of tetragonal PZT.

Experimental data have been acquired using tetragonal single-crystal-like epitaxial PZT layers with low or zero density of extended defects such as threading and/or misfit dislocations.[43,44] This has been done under the belief that it is not appropriate to compare results or to apply models developed for polycrystalline films to single-crystal epitaxial films or vice versa. Especially in the case of the dielectric response, when the microstructure might play a crucial role, any defect can have a contribution to the static dielectric constant. The intrinsic dielectric constant of any material should be basically measured on high-quality single-crystal samples. Otherwise, the results will depend on the quality of the sample, leading to a large spread in values and faulty conclusions. This is the reason why great efforts were made to grow epitaxial layers free from extended structural defects, including misfit or threading dislocations. However, point defects such as oxygen or lead vacancies and inherent impurities of the raw materials of the target used for pulsed laser deposition (PLD) could not be avoided.

We will show first, by comparing the results of the polarization hysteresis measurements and capacitance-voltage (*C*-*V*) characteristics, that the Schottky model is the option for the metal-epitaxial PZT interface. Then, capacitance-frequency (*C*-*f*) and conductance-frequency (*G*-*f*) data acquired under conditions of saturated polarizations and field-independent dielectric constant are simulated using a realistic model for the equivalent circuit, including the capacitance of the Schottky contact and the effective concentration of trap centers associated with point defects. It is shown that, in the absence of 90° domains, the dielectric constant estimated using Eq. (1) is dominated by the extrinsic contributions coming from the Schottky contacts and point defects. The thickness dependence occurs to be an artifact of using Eq. (1) for a structure which is not a simple plane-parallel capacitor. The intrinsic contribution ε_i^* is estimated from simulations

and is then compared to the results of theoretical estimations and Raman measurements. The extrinsic contributions of the electrode interfaces, traps, and 90° domains to the global value of the dielectric constant are also estimated.

II. SAMPLE PREPARATION AND EXPERIMENTAL METHODS

$Pb(Z_{0.2}Ti_{0.8})O_3$ films were prepared by PLD on STO substrates. First, an epitaxial layer of $SrRuO_3$ (SRO) was deposited, serving as bottom electrode and epitaxial template for the growth of the PZT film. The PZT composition was selected for its very good lattice fit with the SRO-STO substrate.[43,44] The MFM structure was achieved by the deposition of the top electrodes through a shadow mask. These were from SRO, deposited by PLD at room temperature, followed by a sputtered Pt layer for visualization. The area of the top contact was 0.09 mm^2.

Using the same deposition conditions, PZT20/80 layers with thicknesses in the 10–250 nm range were grown on the same type of substrates, in order to investigate the thickness dependence of the dielectric constant. The structural quality was investigated by transmission electron microscopy (TEM). It was confirmed that the films are epitaxial, with very clean and sharp interfaces and with a low or zero density of extended defects—i.e., misfit and/or threading dislocations.[43,44] TEM analysis does not give any indications to the existence of a defective dead layer at the electrode-PZT interface. The content of the 90° domains was checked by piezoresponse force microscopy (PFM), and it was found to be negligible up to thicknesses of about 200 nm. By careful manipulation of the substrate processing and growth conditions it was possible to obtain films of about the same thickness, but with different contents of 90° domains. This fact allowed us to evidence the contribution of the movement of 90° domains to the static dielectric constant.

Ferroelectric properties were determined by hysteresis measurements using a ferroelectric analyzer (TF2000, Aix-ACCT). The capacitance measurements and capacitance-voltage characteristics were performed with a HP 4194A impedance/gain analyzer.

III. EXPERIMENTAL RESULTS

A. Hysteresis loop and *C-V* characteristics

In order to extract the dielectric constant, the general practice is to perform the capacitance measurement at low frequencies, usually at 1 kHz, with no applied electric dc field and with small amplitudes for the ac probing signal (50–100 mV). Then, knowing the geometrical dimensions of the capacitor, the value for the relative permittivity ε is calculated using Eq. (1). The main drawback of this procedure is the not-well-defined polarization state, especially for a fresh contact. In this case, the definition of the dielectric constant gives[45]

$$\varepsilon = \frac{1}{\varepsilon_0}\frac{\partial D}{\partial E} = \varepsilon^* + \frac{1}{\varepsilon_0}\frac{\partial P_S}{\partial E}, \tag{2}$$

where D is the electric induction or displacement, E is the electric field, P_S is the dipolar polarization (or spontaneous

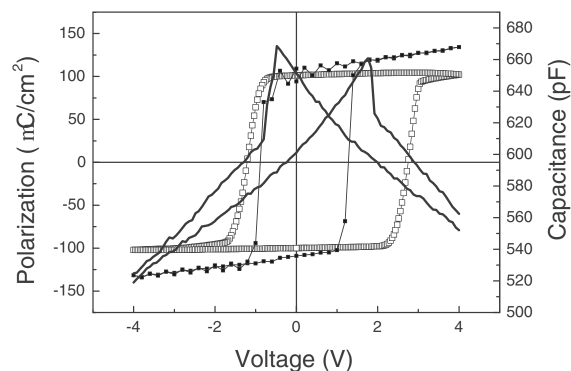

FIG. 1. Hysteresis loop and *C-V* characteristics for a PZT20/80 epitaxial film with a thickness of 215 nm.

polarization) existing in the absence of the electric field, but depending on it in the form of the hysteresis loop, and ε^* is the notation for the linear part of the dielectric constant ε. Equation (2) separates the linear part of the dielectric response from the nonlinear response of the pure ferroelectric polarization.

It can be seen from Eq. (2) that, if the ferroelectric polarization is saturated and if the ferroelectric loop is rectangular, then the term $\partial P_S/\partial E$ is zero and the dielectric constant ε is equal to the linear part ε^*. If the polarization state is not well defined or the loop is not rectangular, then the term $\partial P_S/\partial E$ is nonzero and gives a nonlinear, field-dependent contribution to ε.

Assuming a rectangular hysteresis loop and knowing that the quantity recorded during the hysteresis measurement is in fact D, it occurs that the field dependence of D, when P_S is saturated, should be a straight line. The first consequence of this behavior is that the capacitance of the sample should be constant in the voltage range corresponding to polarization saturation. Therefore, for an ideal insulator or a fully depleted film the *C-V* characteristics should be flat (constant capacitance) in this voltage range, if Eq. (1) applies.

Figure 1 shows the results of the ferroelectric hysteresis and *C-V* measurements performed on the same device of a PZT film. Both the static and dynamic hysteresis loops are presented. It can be observed that the dynamic hysteresis loop is rectangular, with sharp switching and flat saturated polarization. We will not comment on the polarization value, which is rather high even compared with theoretical values.[3] We will just mention that values of about 100 $\mu C/cm^2$ were also reported earlier.[46,47] The static hysteresis loop shows the same polarization values, although the coercive voltages are much smaller than in the case of the dynamic hysteresis, but approximately the same as in the *C-V* characteristic. This problem will not be detailed, as it is not the subject of the paper. However, we draw attention to the fact that, after switching, the "polarization" recorded in the static measurement has a linear dependence on voltage. Recalling that in fact the recorded quantity is the displacement D, it is clear that after switching and saturation of the ferroelectric polarization, according to Eq. (2), the dependence of D on voltage should be linear. According to the same equation the dielectric constant should be practically field independent in this

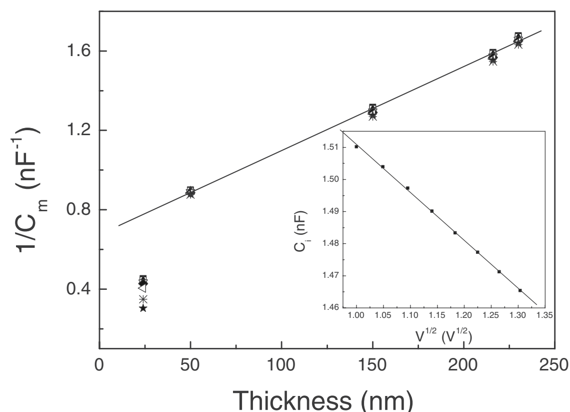

FIG. 2. The dependence of the reverse measured capacitance $1/C_m$ on the film thickness d, for several voltages in the voltage range where the ferroelectric polarization is saturated. The interface capacitance C_i can be evaluated from the intercept. The inset shows the linear dependence of the interface capacitance C_i on the square of the applied voltage V.

field regime, leading to a constant capacitance with voltage. However, the *C-V* characteristics show a continuous voltage variation of the capacitance even after saturation of the ferroelectric polarization.

The above results—i.e., rectangular hysteresis shape and the *C-V* characteristics—as well as the calculation of Zubko *et al.*[48] suggest that the MFM structure cannot be treated as a simple plane-parallel capacitor with the ferroelectric as an ideal insulator or fully depleted semiconductor. The voltage-dependent capacitance, which is characteristic for Schottky contacts, should be considered at the two electrode interfaces.

In order to rule out the applicability of the dead-layer model in our case, we performed *C-V* measurements on films with different thicknesses. We have applied the model of series capacitors for several voltages in the voltage range where the polarization is saturated. The basic relation for the series capacitor model is[34]

$$\frac{1}{C_m} = \frac{1}{C_i} + \frac{d}{\varepsilon_0 \varepsilon A}, \tag{3}$$

where C_m is the measured capacitance, C_i is an interfacial capacitance, and ε is given by Eq. (2). The approximation is that the thickness of the interface capacitance is negligible compared to the thickness of the film. According to Eq. (3), the plot of $1/C_m$ as a function of thickness should be a straight line. The intercept will give the interface capacitance. The $1/C_m \sim d$ representation is shown in Fig. 2 for thicknesses between 24 and 230 nm. Except for the sample with 24 nm thickness, the other points lie well on a straight line. The representation was performed for different voltages outside the voltage domain where the polarization switching takes place; thus, the ferroelectric polarization is assumed saturated. According to Eq. (2), the dielectric constant should be voltage independent. However, according to Fig. 1, the measured capacitance is still voltage dependent. Referring to Eq. (3), the only quantity that can be voltage dependent is the interface capacitance. Thus, we have evaluated the C_i from the intercept of the $1/C_m \sim d$ representation for the other thicknesses (except 24 nm) at different voltages. Plotting C_i as a function of $V^{1/2}$ (see inset of Fig. 2) gives a straight line with a negative slope near unity. This result suggests that the interface capacitance has a voltage dependence similar to that of a Schottky contact. We conclude that the Schottky model is the most suitable to our epitaxial structures. The 24-nm-thick film, which has not been included in the above analysis, confirms this conclusion, as in this case the thickness of the film is comparable to the thickness of the depletion region. Equation (3) is no longer valid in this case, as it is based on the assumption that the depletion thickness is negligible compared to the film thickness. An important consequence of the above discussion is that the PZT films are partly depleted. This is in contrast to previous reports, which consider fully depleted films.[49,50] Contradictory results, regarding partial or full depletion, were also reported for BST.[51,52] It seems to us that the state of partial or full depletion is not an intrinsic property of a ferroelectric film, but is a consequence of several factors, among which are the abundance of structural defects, the quality of the interfaces, the dopant concentration, the film thickness, etc. A second consequence of the above-presented results is that the thickness of the depletion region is about 10 nm or less.

We are aware of a major concern related to the limited applicability of the Schottky model for the capacitance of a metal-semiconductor contact. The approximation of abrupt depletion was developed for a semi-infinite semiconductor with a Schottky contact; thus, the Schottky model is valid if the depletion width at zero bias is considerably smaller than the film thickness.[42] If the depletion width is comparable with the film thickness, then the film becomes fully depleted at very low voltages and the capacitance becomes voltage independent. The Schottky model is no longer valid in this case. Our results suggest that the depletion width at zero is considerable smaller than the film thickness for the investigated thicknesses range; therefore, we assume that the Schottky model applies.

It is worth noting that the Schottky model for the capacitance of a Schottky contact is different to "Schottky model" referring to the thermionic emission over the potential barrier, known also as Schottky emission, and should not be confused. Basically, Schottky emission can be present either or not the film is fully depleted. The difference between partly or fully depleted in this case resumes to an evaluation of the electric field to be used in the current density equation. If the film is fully depleted, then the electric field is constant and is given by the ratio between the applied voltage and the film thickness. If the film is partly depleted, then the field should be the maximum field at the Schottky contact.[42] The Schottky emission can be interface limited or bulk limited, depending on the magnitude of the electron mean free path. As discussed recently by Scott,[2,53] the Schottky model is valid if the electron mean free path is higher than the film thickness, while the Simmons-modified Schottky model is valid when mean free path is smaller than the film thickness. In the first case the electrons are not scattered within the film and their energy is conserved. In the second case the electrons suffer multiple scattering and the energy is not con-

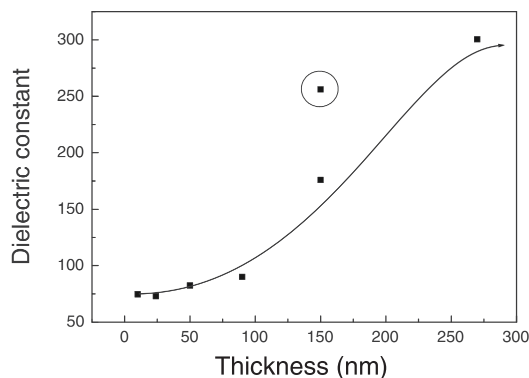

FIG. 3. Thickness dependence of the global dielectric constant, calculated using Eq. (1) for the MFM structure. The line is only to guide the eye.

served. In fact, these are the extreme cases of the thermionic emission-diffusion theory develop by Crowell and Sze.[54] The mean free path of the electron can be estimated using Eq. (3.7) of Scott's text book.[2] Although it has no relation to the topic of the present study, we have estimated the mean free path for our single-crystal-like epitaxial PZT films and we obtained a value of about 20 nm, knowing that the breakdown field is about 50 MV/m and the potential barrier between SRO and PZT20/80 is about 1 eV. This mean free path is smaller than the film thickness for most of our films; thus, it might be that the Simmons equation applies in this case. This fact has no impact on the capacitance used to extract the dielectric constant and will not be further detailed.

B. Thickness dependence of the dielectric constant

The thickness dependence of the dielectric constant, calculated using Eq. (1) and the measured capacitance at zero field, is presented in Fig. 3. The graph includes the samples with negligible density of 90° domains. The encircled point is for a sample with considerable density of 90° domains. The line is a guide for the eye to show that the dielectric constant has the tendency to converge towards some constant value both at high and low thicknesses. The high-thickness value is around 300, while the low-thickness value is about 73. It has to be noticed that the last value is remarkably close to the theoretical value calculated for a stress-free, PZT single crystal of the same composition.[3] Also, the value for high thickness agrees well with other reports[9,11] despite the fact that the extrinsic contributions might be different due to different microstructures. Similar thickness dependences were observed by other authors,[24,25] although on films deposited by chemical routes and having different compositions.

A large difference between the samples without and with 90° domains can be observed although the films have the same thickness. This aspect will be discussed later in more detail.

C. Frequency dependence of the capacitance

The frequency measurements were performed between 1 kHz and 1 MHz on pre-poled devices. The polarization was saturated and, in this way, the contribution of the nonlinear term in Eq. (2) was negligible, considering the shape of the hysteresis loop and the discussion from Sec. III A. Typical C-f and G-f characteristics are shown in Fig. 4. The behavior is similar for all the samples, no matter which thickness or which content of the 90° domains. The capacitance decreases with frequency, while the ac conductance increases. The fact that the ac conductance is not zero, when extrapolating to zero frequency, is due to the presence of the dc leakage. Similar frequency behavior was reported for the dielectric constant in the case of PZT films, although the composition and the microstructure were different.[55–57]

IV. DISCUSSION

A. Model of equivalent circuit for the MFM structure with epitaxial PZT layer

For long time the ferroelectric films with metal electrodes were modeled as a simple capacitance-resistance (R-C) parallel circuit, in which the equivalent resistance takes into consideration the finite losses in the ferroelectric material (dc leakage or ac relaxation mechanisms). This model was used to simulate the hysteresis loop or the C-V characteristic.[58–61] However, different model circuits for the MFM structure were used to explain the current-voltage (I-V) characteristic. Some of them have considered the Schottky rectifying contact in order to explain the dc leakage current behavior.[62–64] Recently, a constant phase element (CPE) was introduced into the equivalent circuit in order to explain the results of impedance measurements on a number of polycrystalline and amorphous materials with high dielectric constant.[56,65–68] As these studies were performed on highly disordered systems, and considering that our PZT films are of single-crystal quality, the presence of a CPE in the equivalent circuit will not be considered.

The discrepancy between the equivalent circuits used for hysteresis and C-V characteristics on the one hand and I-V characteristics on the other hand is mainly due to the fact that ferroelectric properties, like polarization switching and the dielectric constant, are analyzed separately from the charge transport properties. A complete equivalent circuit should consider all necessary elements in order to be applicable to all electric measurements performed on MFM structures, including C-f and G-f characteristics.

Therefore, we have included a Schottky-type capacitance into the equivalent circuit. The Schottky capacitance models the voltage-dependent depletion layers which are present at the electrode interfaces. As any capacitance, the Schottky depletion region can be represented as a parallel C-G connection;[21] therefore, the equivalent circuit of the MFM structure will include the Schottky capacitance C_S, which takes into consideration the equivalent capacitance of both Schottky interfaces; a dc conductance G_{dc}, which takes into consideration the nonzero leakage current at zero frequency and which is dominated by the low conductance of the depleted region; a parallel capacitance-conductance (C_0-G_0) group, taking into consideration the neutral volume, and a serial resistance R_S, taking into consideration the finite resis-

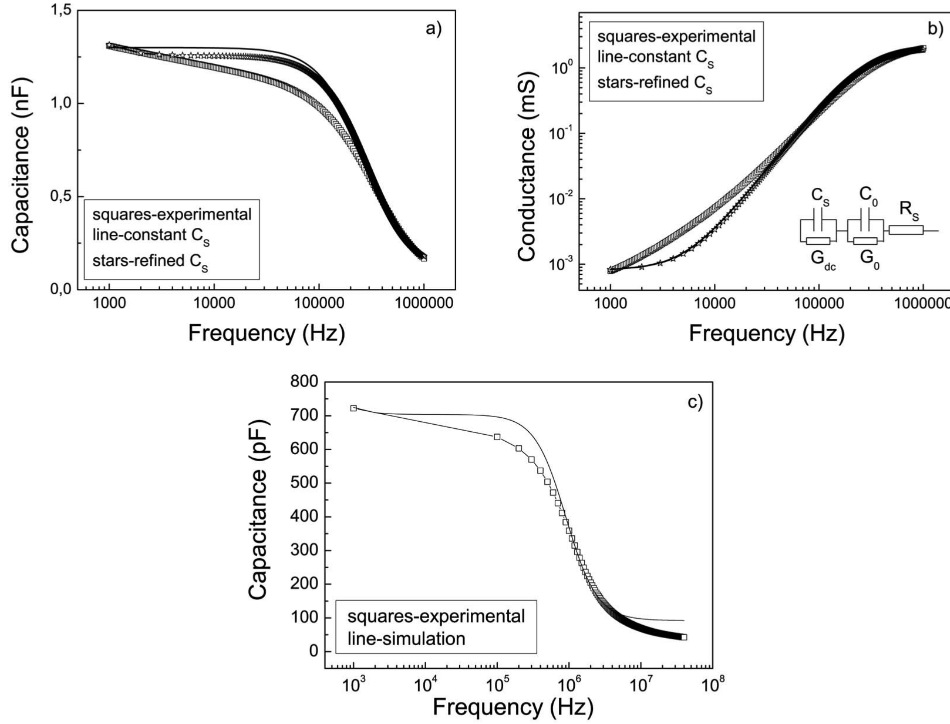

FIG. 4. (a) Capacitance-frequency (C-f) and (b) conductance-frequency (G-f) characteristics of an epitaxial PZT20/80 film with a thickness of 150 nm. The inset in (b) shows the schematic of the equivalent circuit used for simulating the frequency characteristics. The notations stand for C_S, capacitance of the Schottky contact; C_0, capacitance of the neutral ferroelectric layer; G_0, conductance of the neutral ferroelectric layer; R_S, the serial resistance of the SRO electrodes; G_{dc}, the dc conductance of the entire MFM structure. (c) The C-f characteristic up to 40 MHz for a sample of 215 nm. This is to show that the capacitance after relaxation, instead of being constant as shown by simulation, continues to decrease because of the parasitic influences of the external circuitry.

tance of the electrodes. A schematic of the equivalent circuit is shown as an inset in Fig. 4(b).

The link between C_S, C_0, G_0, and R_S on the one hand and the measured capacitance C_m and conductance G_m on the other hand is given by the following equations:

$$C_m = \left(\frac{C_S}{G_{dc}^2+\omega^2 C_S^2}+\frac{C_0}{G_0^2+\omega^2 C_0^2}\right)\left[\left(R_S+\frac{G_{dc}^2}{G_{dc}^2+\omega^2 C_S^2}+\frac{G_0}{G_0^2+\omega^2 C_0^2}\right)^2+\omega^2\left(\frac{C_S}{G_{dc}^2+\omega^2 C_S^2}+\frac{C_0}{G_0^2+\omega^2 C_0^2}\right)^2\right]^{-1}, \quad (4)$$

$$G_m = \left(R_S+\frac{G_{dc}}{G_{dc}^2+\omega^2 C_S^2}+\frac{G_0}{G_0^2+\omega^2 C_0^2}\right)\left[\left(R_S+\frac{G_{dc}}{G_{dc}^2+\omega^2 C_S^2}+\frac{G_0}{G_0^2+\omega^2 C_0^2}\right)^2+\omega^2\left(\frac{C_S}{G_{dc}^2+\omega^2 C_S^2}+\frac{C_0}{G_0^2+\omega^2 C_0^2}\right)^2\right]^{-1}, \quad (5)$$

where $\omega = 2\pi f$, with f the frequency of the small-amplitude ac voltage. The serial resistance R_S of the electrodes can be estimated by measuring the resistance of the SRO layers deposited on STO substrates in the same conditions as the bottom and top electrodes of the present samples. We recall that the bottom electrode is epitaxial while the top electrode is polycrystalline, as the last one was deposited at room temperature. It was found that the resistance of the top electrode is important, which is in the 1–10 Ω range, depending probably on the thickness and microstructure of the SRO layer. Although the number of laser pulses was the same for all samples, the thickness of the SRO layers is not exactly the same, a variation of 20% being possible from sample to sample. The amount of structural defects in the top SRO contact is also variable from sample to sample and can lead to some spread in the values of R_S. We can say that the experimental measurements helped to estimated the order of magnitude for R_S but not the exact value; therefore, this quantity will be further on treated as a parameter bound to values in the same range as the experimental ones. On the other hand, the I-V measurements have shown high current densities in the studied samples, suggesting a relative leaky neutral volume.[69] Considering the experimental results of dc current measurements it can be assumed that the condition $1/G_{dc} \gg (R_S + 1/G_0)$ is fulfilled and that $G_{dc} \to 0$ as is the case for a depleted region. Considering these approximations Eq. (4) can be simplified to

$$C_m = \left(\frac{1}{\omega^2 C_S}+\frac{C_0}{G_0^2+\omega^2 C_0^2}\right)\left[\left(R_S+\frac{G_0}{G_0^2+\omega^2 C_0^2}\right)^2+\left(\frac{1}{\omega C_S}+\frac{\omega C_0}{G_0^2+\omega^2 C_0^2}\right)^2\right]^{-1}. \quad (6)$$

Equation (5) in dc conditions ($\omega = 0$) leads to

$$G_m = \left(R_S + \frac{1}{G_{dc}} + \frac{1}{G_0} \right)^{-1} \sim G_{dc}. \quad (7)$$

The value of G_{dc} was estimated to about 0.8 μS from the experimental G-f graph shown in Fig. 4(b), by extrapolation to zero frequency. Considering Eq. (7), Eq. (5) can be further on simplified by arranging it in two parts: one which controls the high-frequency response, and in which $G_{dc} \rightarrow 0$, and a second part which considers only the dc response and which is approximately equal to G_{dc}:

$$G_m = \left(R_S + \frac{G_0}{G_0^2 + \omega^2 C_0^2} \right) \Bigg[\left(R_S + \frac{G_0}{G_0^2 + \omega^2 C_0^2} \right)^2 + \left(\frac{1}{\omega C_S} + \frac{\omega C_0}{G_0^2 + \omega^2 C_0^2} \right)^2 \Bigg]^{-1} + G_{dc}. \quad (8)$$

We mention that this approximated equation is valid for the specific case of PZT films having a low bulk resistance. If the bulk resistance is comparable with G_{dc}, then the exact equation (5) should be used.

The experimental C-f and G-f dependences shown in Fig. 4 were fitted with the above equations (6) and (8) in order to obtain the parameters C_S, C_0, G_0, and R_S. The best fit was obtained for the following values: C_S=1.3 nF, C_0=150 pF, G_0=2.4 mS, and R_S=4 Ω. It is easily found that the value C_S coincides with the measured capacitance C_m at the lowest frequency, which is 1 kHz in the present case. The other parameters serve to simulate frequency dependences. The results of the simulations, for both the capacitance and conductance, are also shown in Fig. 4. The simulated values are higher than the measured ones for the frequency range between 1 kHz and about 300 kHz. In fact, the simulated capacitance is constant and equal to C_S up to about 100 kHz, then starts to decrease due to the bulk components C_0 and G_0. This is because C_S was considered constant, neglecting the contribution of deep traps in the depleted region, which have also a frequency-dependent response. This aspect will be discussed later on in some detail. We emphasize that the same set of parameters simulates quite well the frequency dependences of both capacitance and conductance, the latter being related to the loss tangent.[21] The above result shows that, at low frequencies, the capacitance of the MFM structure is dominated by interface phenomena. Similar results were recently reported in the case of hexagonal $BaTiO_3$ single crystals.[70] We mention that the simulation with the exact equations (4) and (5) does not bring a better fit in the intermediate frequency range.

One can argue that extending the frequency range for capacitance measurements we should obtain a plateau of constant capacitance equal with C_0. Unfortunately, the parasitic capacitance and inductance of the external wires and intermediate connectors strongly affect the measured capacitance values at frequency higher than 5 MHz. Although efforts were made to reduce the length of the external wires and the number of intermediate connections along the measurement circuit, it was not possible to obtain a clear constant capacitance in the frequency range up to 40 MHz allowed by the HP 4194A impedance/gain analyzer. As seen from Fig. 4(c) the slope of the C-f graph is considerable reduced above 1 MHz, but the capacitance value continues to decrease up to about 40–50 pF at 40 MHz. This capacitance leads to a value of around 13 for the dielectric constant, which is much smaller than any theoretical estimates. For this reason the experimental measurements were performed only in the 1 kHz to 1 MHz frequency range.

B. Intrinsic and extrinsic contributions to the dielectric constant of the MFM structure

Taking the C_0 value as the true capacitance of the PZT layer and using Eq. (1) to calculate the dielectric constant, a value of around 27 is obtained. This value is much smaller than any of the values presented in Fig. 3, even for the thinnest film of 10 nm.

It is interesting to note that the value of 27 for the dielectric constant of PZT20/80, although it is a rough estimate, is close to the value of around 28 estimated for $PbTiO_3$ thin films from Raman measurements[71] and is fairly close to the value of 37 obtained from calculations performed in fixed-strain conditions by using modern theories on ferroelectricity.[5] We recall that a value of 41 was estimated from Raman measurements, using the LST relation in the case of $PbTiO_3$ single crystal.[4]

The use of the LST relation might be a subject of discussion, as it was theoretically shown that even PTO is not a purely displacive ferroelectric. However, at room temperature the displacive character is dominant and only at high temperature and in the paraelectric phase does the order-disorder character become distinct.[72] The mixture between displacive and order-disorder becomes more relevant in the case of PZT films in the morphotropic phase region, for Zr-rich films, or for doped PTO materials.[73,74] As our films are near the PTO end of the PZT phase diagram and are of single-crystal quality, we assume that the displacive character is dominant and that the LST relation still holds. In any case, all of the above-cited values are much smaller than the one predicted by the thermodynamic theory.[3]

Considering all these results, it appears that the intrinsic value of the dielectric constant of epitaxial Ti-rich PZT films is significantly smaller than was previously thought, possibly in the range of 30–40 and not of the order of 200–300 as extracted from a capacitance measurement of MFM structure. The fact that the dielectric constant of the thinnest measured films approaches the intrinsic value supports the idea that, at low thickness, the films become fully depleted. The metal-ferroelectric interface contribution vanishes, and only structural extended or point defects which are electronically active can still have a contribution to the dielectric constant. That might explain the difference from about 30–40, obtained theoretically, to about 70, as shown in Fig. 3. In any case, further studies are needed to obtain the true intrinsic dielectric constant from experimental measurements. These imply on the one hand a strict control of the PZT structure (including point defects) in order to obtain ideal single-crystal films and on the other hand the elimination of any parasitic inductance and capacitance in the external circuit that might affect the capacitance measurement.

We recall that the contribution of the spontaneous polarization to the dielectric constant calculated with Eq. (2) is

considered negligible (the term $\partial P_S/\partial E$ is null). Thus, $\varepsilon = \varepsilon^*$, meaning that the global dielectric constant calculated with Eq. (1) contains only the linear response to the electric field. This global dielectric constant, calculated from the measured capacitance C_m, might contain intrinsic and extrinsic contributions. Considering that the intrinsic contribution is around 30, it results that the global dielectric constant is, in fact, dominated by extrinsic contributions.

Some experiments were performed in order to extract the weight of the possible extrinsic contributions to the dielectric constant. The possible extrinsic contributions are from: (i) deep traps located in the depletion region and (ii) 90° domains, when they are present.

Although the presence of structural defects in PZT films is generally accepted (dislocations, point defects, etc.), their electrical activity by trapping-detrapping charge carriers is usually neglected when discussing the contribution to the dielectric constant. The above model can be refined by introducing the exact expression for the Schottky capacitance C_S, which takes into consideration both the existence of a depletion region at the contact and the presence of deep traps in the interface region. This equation is[75]

$$C_S = \left(\frac{\varepsilon_0 \varepsilon_i N_{\mathrm{dop}}}{2(V+V_{\mathrm{bi}})}\right)^{1/2}\left(1+\frac{N_T}{p(T)}\frac{e_n^2}{e_n^2+\omega^2}\right), \qquad (9)$$

where ε_i is the intrinsic, material characteristic, dielectric constant. N_{dop} is the doping concentration which is considered equal to the free carrier concentration $p(T)$. It is assumed that PZT is a p-type material, and thus the holes are the majority carriers. The same is valid for an n-type material, only changing $p(T)$ in $n(T)$, with $n(T)$ the density of free electrons at temperature T. N_T is the concentration of filled traps in the depletion region, and e_n is the emission coefficient of the traps. This is the reverse of the emission time constant of the traps, $e_n = 1/\tau_n$. V_{bi} is the built-in potential.

Some of the quantities involved in Eq. (9) can be estimated from current-voltage (I-V) and C-V measurements, using the newly developed model for the metal-ferroelectric interface.[43,76] The quantity $p(T) = N_{\mathrm{dop}}$ can be evaluated from the C-V characteristic, while N_T and V_{bi} are extracted from the I-V measurement. The following values were obtained for the studied films: $p(T) \sim (2-6) \times 10^{18}$ cm^{-3}, $N_T \sim (9-10) \times 10^{20}$ cm^{-3}, and $V_{\mathrm{bi}} \sim 0.5$ V. Further on we introduce Eq. (9) into Eqs. (6) and (8) and perform new simulations using the above values as starting numbers. The value of 27 was used for the intrinsic dielectric constant ε_i in Eq. (9). The only not-known parameter is the emission coefficient e_n. For the investigated samples the best fit with the experimental frequency dependences was obtained for e_n values in the 50–100 s^{-1} range. The fit is shown in Fig. 4 for comparison with the experimental data. An emission coefficient of 50–100 s^{-1} gives a time constant of 10–20 ms. This value is characteristic for deep traps in wide-gap semiconductors. PZT can be considered as such, with a gap value of around 3.5 eV.[77] Thus, using the trap-containing equation (9), the frequency response can be better simulated, at least in the low-frequency range. Only one trap level was considered, but in real PZT films there can be more deep traps. The frequency dependence can be even better simulated if the energetic distribution of the traps is known, together with their emission parameters.

Further on, using PFM it was possible to estimate the density of the 90° domains. Two samples of 150 nm thickness were then analyzed, one with a negligible density of 90° domains and the other one with a significant density of 90° domains.

The frequency dependences for the two samples were simulated using expression (9) for the C_S in Eqs. (6) and (8) and using the numerical values mentioned above. For each sample there will be a set of four capacitances: (i) the intrinsic value C_0; (ii) the Schottky capacitance without traps C_S^*, obtained from Eq. (9) by taking N_T null; (iii) the Schottky capacitance with traps C_S, calculated with Eq. (9); (iv) the measured capacitance C_m. Knowing these values at 1 kHz, it is possible to calculate the dielectric constant in different situations using Eq. (1).

For the sample with negligible density of 90° domains the following values were obtained: (i) intrinsic value 27, from $C_0 = 150$ pF; (ii) 150 from $C_S^* = 810$ pF; (iii) 160 from $C_S = 836$ pF; (iv) about 170 from $C_m = 900$ pF. From these values it is clear that the Schottky capacitance brings the dominant extrinsic contribution to the global dielectric constant. The deep traps bring a minor contribution at low frequencies, as well as the few 90° domains which were observed by PFM.

For the sample with a significant density of 90° domains the numbers obtained for the dielectric constants in various situations are (i) intrinsic value 27, from $C_0 = 150$ pF; (ii) about 238 from $C_S^* = 1268$ pF; (iii) 242 from $C_S = 1300$ pF; (iv) about 260 from $C_m = 1380$ pF. Again, the major extrinsic contribution is given by the standard Schottky capacitance. The contribution of C_S^* is larger in the sample with higher density of 90° domains. This fact is somewhat unexpected, considering that the MFM structures were grown in the same conditions, using the same method, and having the same electrodes. From the electronic point of view one may expect to have similar interfaces, with about the same standard Schottky capacitance. However, the effects of the 90° domains, located in the depletion regions, on the overall properties of the Schottky interface are not very well known although some theoretical models were developed for this case.[78] It is assumed that the 90° domain walls are charged; thus, their effect on the space charge density in the depleted region might be significant. The different doping concentrations, 2.5×10^{18} cm^{-3} compared to 5.5×10^{18} cm^{-3} as obtained from C-V measurements, can also explain the difference.

The apparent minor contribution of the 90° domains located in the volume of the film to the global dielectric constant might be explained by the fact that these domains are hardly movable, requesting voltages much larger than the small-amplitude ac signal used for capacitance measurements.[79] The contribution of the 90° domains to the dielectric constant can be increased using special configurations for the top electrode.[80]

Regarding the presence of deep traps in the epitaxial PZT films, this was evidenced by the presence of a short-circuit photovoltaic signal at wavelengths corresponding to subgap

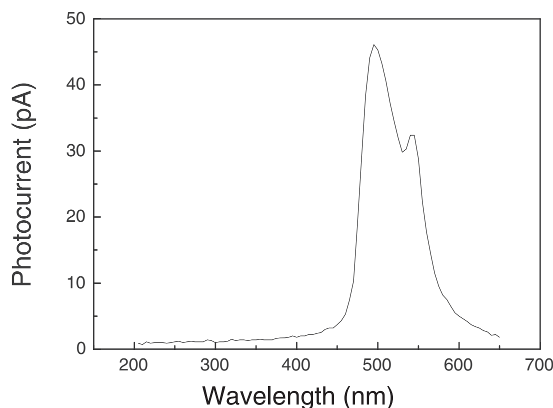

FIG. 5. Spectral distribution of the subgap photovoltaic short-circuit current measured on epitaxial PZT20/80 films.

energies. The reasoning was as follows: If there are deep traps in the PZT, some of them might be filled in the interface region due to the energy band bending. When illuminated with light having enough energy to excite the trapped carrier in the bands, a current should occur in the external circuit due to the electric field existing in the interface regions in the case of Schottky contacts. Therefore, a short-circuit current should be measurable at energies below the gap value, especially if the concentration of trap centers is important. A Xe lamp was used for the experiment, in conjunction with a monochromator and a UV filter cutting down all the wavelengths below 450 nm. These precautions were taken in order to suppress the signal produced by the fundamental absorption of the higher diffraction orders of the UV wavelengths. The recorded current is presented in Fig. 5.

A clear nonzero signal can be observed at wavelengths between 455 and 620 nm. These correspond to energies in the region 2.0–2.7 eV. From these results we can conclude that there are deep trap centers located near the midgap in PZT. As suggested by the continuous spectral distribution shown in Fig. 5, it might be a more or less continuous distribution of traps covering the above-mentioned energy spectrum. The two local peaks suggest the presence of two discrete trapping levels in the same energy range. This result confirms the fact that the frequency response of the deep levels might be more complicated than the simple case considered in simulations, with only one discrete trap level.

C. Thickness dependence of the dielectric constant

The results obtained on the two samples with different densities of 90° domains show that the bulk contribution, giving the intrinsic part of the dielectric constant, is the same. Only the extrinsic contribution has changed. However, the two samples were of similar thickness, 150 nm. The question is how the intrinsic dielectric constant at different thickness behaves.

We performed similar simulations and calculations for a sample of 24 nm thickness, in which the 90° domains are totally absent. The resulting values are C_S=2.7 nF, C_0=900 pF, G_0=39.5 mS, and R_S=10 Ω. The dielectric constant calculated using C_S in Eq. (1) is 80, in fairly good agreement with the value of 75 calculated using C_m. The important point is that the bulk part is thickness independent, giving the same dielectric constant of about 27, while the "global dielectric constant" calculated by Eq. (1) is thickness dependent. This apparent "thickness dependence" shown in Fig. 2 seems to come from the Schottky capacitance associated with the electrode interfaces.

As the thickness of the depleted regions becomes comparable to the thickness of the bulk, the equivalent dielectric constant calculated by Eq. (1) approaches the intrinsic value and thus will decrease with the thickness. If the bulk thickness is much larger than the depleted regions, then the dielectric constant will converge towards a value which is controlled by bulk extrinsic contributions, such as 90° domains or dislocations. These will form in larger amounts in thicker films, it being known that above some critical thickness the strain imposed by the substrate will relax by forming extended structural defects.

The results of the C-f measurements and the conclusion that the intrinsic dielectric constant of the PZT material is thickness independent are supported by the results of PFM investigations regarding the piezoelectric coefficient d_{33}. It is known that in tetragonal ferroelectrics with cubic paraelectric phase the piezoelectric coefficient, the dielectric constant, and the spontaneous polarization P_S are related through the equation[81–83]

$$d_{33} = 2Q\varepsilon_0\varepsilon_{33}P_S, \tag{10}$$

where Q is the electrostriction coefficient. In the investigated thickness range from 24 nm up to 270 nm, all our samples possess a spontaneous polarization of 1 ± 0.1 C/m^2. The d_{33} value estimated from the first harmonic of the PFM signal[84,85] is 60 ± 5 pm/V and shows no thickness dependence in the investigated thickness range (Fig. 6). The values were determined in uniform field by performing PFM measurements through the top electrode, improving also the contact between the PFM tip and the surface.[58] The obtained values are in good agreement with other reports.[86,87] Considering that Q is also a material constant and should be thickness independent, it results that the value of the dielectric constant ε_{33} should be also thickness independent. The electrostrictive coefficient can be related to the tetragonality and polarization by the relation[88,47]

$$\frac{c}{a} - 1 = QP_S^2. \tag{11}$$

The tetragonality of the PZT films was calculated from the electron diffraction pattern (TEM), $c/a \sim 1.06$ for all thicknesses from 20 nm to 270 nm. The tetragonality of the cubic, paraelectric phase was assumed to be 1, as the lattice mismatch is negligibly small and the PZT film grows in nonstrained conditions. Knowing c/a and P_S ($\sim$1 C/m^2), which are thickness independent for the investigated range of thickness, Q could be calculated by Eq. (11), $Q \sim 0.06$ m^4/C^2. This value is in between other reported values, such as 0.025 m^4/C^2 (Ref. 89) or 0.089 m^4/C^2 (Ref. 3).

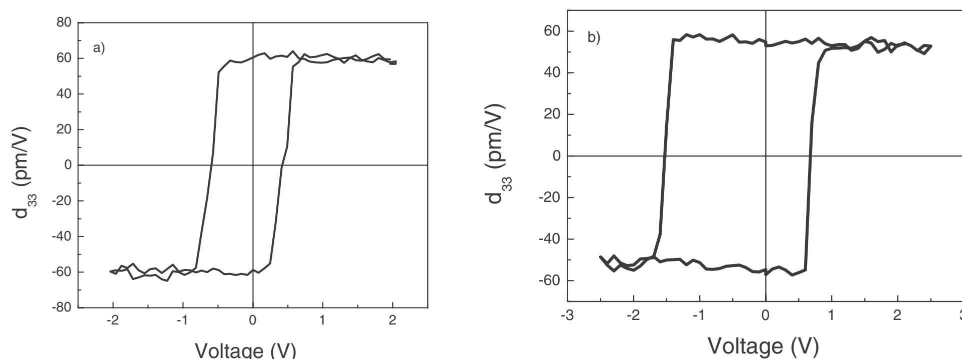

FIG. 6. PFM hysteresis loops for d_{33}. (a) Film with the thickness of 24 nm and (b) film with a thickness of 230 nm. The amplitude of the 10 kHz ac voltage used for the measurement was 0.5 V in both cases.

Using the above-mentioned values for d_{33}, Q, and P_S in Eq. (10), a value of about 56 results for the dielectric constant. If the theoretical value of 0.089 m^4/C^2 is used, Eq. (10), instead of the experimental one determined from Eq. (11), then the value for the dielectric constant is about 38. Both values are smaller than calculated from the measured capacitance C_m and are closer to the dielectric constant estimated from the *C-f* simulations. In any case, the PFM results confirm that the thickness dependence of the dielectric constant is an effect of extrinsic phenomena related to the overall MFM structure and is not an intrinsic property of the PZT material.

V. CONCLUSIONS

From the above presented results the following can be concluded.

(i) The "dielectric constant" calculated by Eq. (1) is controlled by extrinsic effects related to the presence of the Schottky contacts, trap centers or/and 90° domains.

(ii) The epitaxial tetragonal PZT films are only partly depleted.

(iii) The dielectric behavior at low frequencies is dominated by the above mentioned extrinsic contributions.

(iv) The intrinsic part of the global dielectric constant appears to be thickness independent, as it should be for a true material constant.

(v) The so-called thickness dependence of the dielectric constant is an artifact originating in an incorrect use of Eq. (1) for the case of a MFM structure comprising Schottky interface capacitances, as is the case of tetragonal PZT films with SRO electrodes.

(vi) The above model might not be directly applicable for polycrystalline ferroelectric films or ferroelectrics with high ionic degree of bonding such as $BaTiO_3$ or BST.

ACKNOWLEDGMENTS

This work was partly supported by the Volkswagen Stiftung under Contract No. I/77738 and by the CEEX program (Romanian Ministry of Education and Research) under the Project No. DINAFER-2-CEEX-06-11-44.

[1] K. Uchino, *Ferroelectric Devices* (Marcel Dekker, New York, 2000).
[2] J. F. Scott, in *Advanced Microelectronics Series*, edited by K. Itoh and T. Sakurai (Springer-Verlag, Berlin, 2000).
[3] M. J. Haun, E. Furman, S. J. Jang, and L. E. Cross, Ferroelectrics **99**, 63 (1989).
[4] J. A. Sanjurjo, E. Lopez-Cruz, and G. Burns, Phys. Rev. B **28**, 7260 (1983).
[5] N. Sai, K. M. Rabe, and D. Vanderbilt, Phys. Rev. B **66**, 104108 (2002).
[6] P. Ghosez (private communication).
[7] M. Klee, R. Eusemann, R. Waser, W. Brand, and H. van Haal, J. Appl. Phys. **72**, 1566 (1992).
[8] T. Oikawa, M. Aratani, K. Funakubo, K. Saito, and M. Mizuhira, J. Appl. Phys. **95**, 3111 (2004).
[9] S. Yokoyama, Y. Honda, H. Morioka, S. Okamotot, H. Funakubo, T. Iijima, H. Matsuda, K. Saito, T. Yamamoto, H. Okino, O. Sakata, and S. Kimura, J. Appl. Phys. **98**, 094106 (2005).
[10] R. Takayama and Y. Tomita, J. Appl. Phys. **65**, 1666 (1989).
[11] C. M. Foster, G. R. Bai, R. Csencsits, J. Vetrone, R. Jammy, L. A. Wills, E. Carr, and J. Amanao, J. Appl. Phys. **81**, 2349 (1997).
[12] G. Burns and B. A. Scott, Solid State Commun. **13**, 417 (1973).
[13] G. Burns, Phys. Rev. B **13**, 215 (1976).
[14] G. Burns and E. Burstein, Ferroelectrics **7**, 297 (1974).
[15] D. K. Schroeder, *Semiconductor Material and Device Characterization* (Wiley-Interscience, New York, 1998).
[16] N. A. Pertsev, G. Arlt, and A. G. Zembilgotov, Phys. Rev. Lett. **76**, 1364 (1996).
[17] N. A. Pertsev and A. Yu. Emelyanov, Phys. Rev. B **65**, 174115 (2002).
[18] F. Xu, S. Trolier-McKinstry, W. Ren, B. Xu, Z. L. Xie, and K. J. Hemker, J. Appl. Phys. **89**, 1336 (2001).
[19] A. Fouskova, J. Phys. Soc. Jpn. **20**, 1625 (1965).
[20] J. Fousek, Czech. J. Phys., Sect. A **15**, 412 (1965).
[21] A. K. Jonscher, *Dielectric Relaxation in Solids* (Chelsea Dielectrics Press, London 1983).

[22] J. M. Wesselinowa, S. Trimper, and K. Zabrocki, J. Phys.: Condens. Matter **17**, 4687 (2005).
[23] K. R. Udayakumar, P. J. Schuele, J. Chen, S. Krupanidhi, and L. E. Cross, J. Appl. Phys. **77**, 3981 (1995).
[24] S. H. Kim, H. J. Woo, J. Ha, C. S. Hwang, H. R. Kim, and A. I. Kingon, Appl. Phys. Lett. **78**, 2885 (2001).
[25] J. F. Scott, D. Galt, J. C. Price, J. A. Beall, R. H. Ono, C. A. Paz de Araujo, and L. D. McMillan, Integr. Ferroelectr. **6**, 189 (1995).
[26] S. Iakovlev, C. H. Solterbeck, and M. Es-Souni, Appl. Phys. Lett. **81**, 1854 (2001).
[27] R. Bouregba, G. Le Rhun, G. Poullain, and G. Leclerc, J. Appl. Phys. **99**, 034102 (2006).
[28] X. J. Meng, J. L. Sun, J. Yu, L. X. Bo, C. P. Jiang, Q. Sun, S. L. Guo, and J. H. Chu, Appl. Phys. Lett. **78**, 2548 (2001).
[29] C. Zhou and D. M. Newns, J. Appl. Phys. **82**, 3081 (1997).
[30] K. Natori, D. Otani, and N. Sano, Appl. Phys. Lett. **73**, 632 (1998).
[31] Y. Zheng, B. Wang, and C. H. Woo, Appl. Phys. Lett. **88**, 092903 (2006).
[32] A. M. Bratkovsky and A. P. Levanyuk, Phys. Rev. Lett. **94**, 107601 (2005).
[33] M. M. Saad, P. Baxter, R. M. Bowman, J. M. Gregg, F. D. Morrison, and J. F. Scott, J. Phys.: Condens. Matter **16**, L451 (2004).
[34] A. Lookman, R. M. Bowman, J. M. Gregg, J. Kut, S. Rios, M. Dawber, A. Ruediger, and J. F. Scott, J. Appl. Phys. **96**, 555 (2004).
[35] M. M. Saad, R. M. Bowman, and J. M. Gregg, Appl. Phys. Lett. **84**, 1159 (2004).
[36] K. Igarashi, K. Koumoto, and H. Yanagida, J. Mater. Sci. **22**, 2828 (1987).
[37] R. E. Cohen, Nature (London) **358**, 136 (1992).
[38] L. Despont, C. Koitzsch, F. Clerc, M. G. Garnier, P. Aebi, C. Lichtensteiger, J.-M. Triscone, F. J. Garcia de Abajo, E. Bousquet, and Ph. Ghosez, Phys. Rev. B **73**, 094110 (2006).
[39] L. Lee, C. H. Choi, B. H. Park, T. W. Noh, and J. K. Lee, Appl. Phys. Lett. **72**, 3380 (1998).
[40] H. Matsuura, New J. Phys. **2**, 8.1 (2000).
[41] L. Pintilie and M. Alexe, J. Appl. Phys. **98**, 124103 (2005).
[42] S. M. Sze, *Physics of Semiconductor Devices*, 2nd ed. (Wiley, New York, 1981).
[43] I. Vrejoiu, G. Le Rhun, L. Pintilie, D. Hesse, M. Alexe, and U. Gösele, Adv. Mater. **18**, 1657 (2006).
[44] I. Vrejoiu, G. Le Rhun, N. D. Zakharov, D. Hesse, L. Pintilie, and M. Alexe, Phil. Mag. **86**, 4477 (2006).
[45] M. E. Lines and A. M. Glass, *Principles and Applications of Ferroelectrics and Related Materials* (Clarendon Press, Oxford, 1977).
[46] H. Morioka, G. Asano, T. Oikawa, H. Funakubo, and K. Saito, Appl. Phys. Lett. **82**, 4761 (2003).
[47] H. Morioka, S. Yokoyama, T. Oikawa, H. Funakubo, and K. Saito, Appl. Phys. Lett. **85**, 3516 (2004).
[48] P. Zubko, D. J. Jung, and J. F. Scott, J. Appl. Phys. **100**, 114112 (2006).
[49] J. C. Shin, C. S. Hwang, H. J. Kim, and S. O. Park, Appl. Phys. Lett. **75**, 3411 (1999).
[50] G. W. Dietz and R. Waser, Thin Solid Films **299**, 53 (1997).
[51] C. Hwang, B. T. Lee, C. S. Kang, K. H. Lee, H. Cho, H. Hideki, W. D. Kim, S. I. Lee, and M. Y. Lee, J. Appl. Phys. **85**, 287 (1999).
[52] G. W. Dietz, M. Schumacher, R. Waser, S. K. Streiffer, C. Basceri, and A. I. Kingon, J. Appl. Phys. **82**, 2359 (1997).
[53] J. F. Scott, J. Phys.: Condens. Matter **18**, R361 (2006).
[54] C. R. Crowell and S. M. Sze, Solid-State Electron. **9**, 1035 (1965).
[55] Y. J. Song, Y. Zhu, and S. B. Desu, Appl. Phys. Lett. **72**, 2686 (1998).
[56] Z. G. Zhang, D. P. Chu, B. M. McGregor, P. Migliorato, K. Ohashi, K. Hasegawa, and T. Shimoda, Appl. Phys. Lett. **83**, 2892 (2001).
[57] J. Cheng, W. Zhu, N. Li, and L. E. Cross, J. Appl. Phys. **91**, 5997 (2002).
[58] S. L. Miller, R. D. Nasby, J. R. Schwank, M. S. Rodgers, and P. V. Dressendorfer, J. Appl. Phys. **68**, 6463 (1990).
[59] F. Chai, J. Brews, R. Schrimpf, and D. Birnie, J. Appl. Phys. **78**, 4766 (1995).
[60] D. B. A. Rep and M. J. W. Prins, J. Appl. Phys. **85**, 7923 (1999).
[61] R. Bouregba and G. Poullain, J. Appl. Phys. **93**, 522 (2004).
[62] J. F. Scott, Ferroelectrics **232**, 25 (1999).
[63] S. Dey, P. Alluri, and J. Lee, Integr. Ferroelectr. **7**, 341 (1995).
[64] R. Bouregba, G. Poullain, B. Vilquin, and G. Le Rhun, J. Appl. Phys. **93**, 5583 (2003).
[65] E. J. Abram, D. C. Sinclair, and A. R. West, J. Electroceram. **10**, 165 (2003).
[66] D. Szwagierczak and J. Kulawik, J. Eur. Ceram. Soc. **24**, 1979 (2004).
[67] G. P. Choi, J. H. Park, C. H. Lee, I. D. Kim, and H. G. Kim, Jpn. J. Appl. Phys., Part 1 **39**, 5151 (2000).
[68] O. K. Tan, X. F. Chen, and W. Zhu, J. Mater. Sci. **38**, 4353 (2003).
[69] L. Pintilie, I. Vrejoiu, D. Hesse, G. LeRhun, and M. Alexe, Phys. Rev. B **75**, 104103 (2007).
[70] J. Yu, T. Ischikawa, Y. Arai, S. Yoda, M. Itoh, and Y. Saita, Appl. Phys. Lett. **87**, 252904 (2005).
[71] Yu. I. Yuzyuk, R. Farhi, V. L. Lorman, L. M. Rabkin, L. A. Sapozhnikov, E. V. Sviridov, and I. N. Zakharachenko, J. Appl. Phys. **84**, 452 (1998).
[72] Y. H. Shin, V. R. Cooper, I. Grinberg, and A. M. Rappe, Phys. Rev. B **71**, 054104 (2005).
[73] T. Y. Kim, H. M. Jang, and S. M. Cho, J. Appl. Phys. **91**, 336 (2002).
[74] R. V. Vedrinskii, E. S. Nazarenko, M. P. Lemeshko, V. Nassif, O. Proux, A. A. Novakovich, and Y. Joly, Phys. Rev. B **73**, 134109 (2006).
[75] G. Vincent, D. Bois, and P. Pinard, J. Appl. Phys. **46**, 5173 (1975).
[76] L. Pintilie, I. Boerasu, M. J. M. Gomes, T. Zhao, R. Ramesh, and M. Alexe, J. Appl. Phys. **98**, 124104 (2005).
[77] I. Pintilie, L. Pintilie, K. Irmscher, and B. Thomas, Appl. Phys. Lett. **81**, 4841 (2002).
[78] Y. Xiao, V. B. Shenoy, and K. Bhattacharya, Phys. Rev. Lett. **95**, 247603 (2005).
[79] V. Nagarajan, A. Roytburd, A. Stanishevsky, S. Prasertchoung, T. Zhao, L. Chen, J. Melngailis, O. Auciello, and R. Ramesh, Nat. Mater. **2**, 43 (2003).
[80] G. Le Rhun, I. Vrejoiu, L. Pintilie, D. Hesse, M. Alexe and U. Gösele, Nanotechnology **17**, 3154 (2006).
[81] C. Harnagea, A. Pignolet, M. Alexe, D. Hesse, and U. Gösele, Appl. Phys. A: Mater. Sci. Process. **70**, 261 (2000).

[82] D. Damjanovic, Rep. Prog. Phys. **61**, 1267 (1998).
[83] A. F. Devonshire, Philos. Mag. **42**, 1065 (1951).
[84] C. Harnagea, Ph.D. thesis, Martin Luther University, Halle, Germany, 2000.
[85] G. Zavala, J. H. Fendler, and S. Trolier-McKinstry, J. Appl. Phys. **81**, 7480 (1997).
[86] O. Kuffer, I. Maggio-Aprile, J.-M. Triscone, O. Fischer, and Ch. Renner, Appl. Phys. Lett. **77**, 1701 (2000).
[87] Jun Ouyang, S. Y. Yang, L. Chen, R. Ramesh, and A. L. Roytburd, Appl. Phys. Lett. **85**, 278 (2004).
[88] F. Jona and G. Shirane, *Ferroelectric Crystals* (Dover, New York, 1993).
[89] V. Nagarajan, I. G. Jenkins, S. P. Alpay, H. Li, S. Aggarwal, L. Salamanca-Riba, A. L. Roytburd, and R. Ramesh, J. Appl. Phys. **86**, 595 (1999).